

Physics Based Modeling of Turbulent Heat Flux in Shock Dominated Flows

By R. Quadros† AND K. Sinha‡

Department of Aerospace Engineering, Indian Institute of Technology Bombay, Mumbai

Interaction of a purely vortical isotropic turbulence with a normal shock wave is considered for analysis. Theoretical tool called Linear Inviscid Analysis (LIA) is used for studying this canonical shock turbulence problem. R_{uT} which represents the normalized turbulent heat flux, is studied in the region downstream of the shock for a range of upstream Mach numbers. DNS data available from literature for similar configuration is used as benchmark for comparison. Effect of M_t and Re_λ on generation and evolution of R_{uT} is studied from DNS data and compared with LIA results. Finally, the effect of upstream energy spectrum shape on prediction of R_{uT} is analyzed.

1. Introduction

Shock-boundary layer interaction is commonly seen in high speed flows and is an important phenomenon. In the region of such interactions, high wall pressure and wall heat flux is observed along with topological changes such as boundary layer separation [1]. Accurate prediction of these high aero-thermal loads is important from a design point of view. Numerical simulation of such flows of engineering interest largely relies on Reynolds Averaged Navier Stokes (RANS) equations.

RANS equations solve for the mean flow variables. The effect of turbulence on the mean flow is modeled in terms of suitable constants and mean flow variable gradients. Conventional RANS models incorrectly predict the wall heat flux in the region of shock-boundary layer interaction [2]. This indicates to additional physics that is uncaptured by RANS models and is a cause for further investigation.

An important term in Reynolds averaged compressible energy conservation equation is the turbulent heat flux vector $\overline{u_j'' h''}$ where u_j'' and h'' represent the Favre fluctuation in x_j directional velocity and enthalpy respectively. Tilde denotes Favre averaging. In the linear limit considered in this work, $\overline{u_j'' h''} = \overline{u_j' h'}$ where overbar represents Reynolds averaging and u_j' and h' represent Reynolds fluctuation in velocity and enthalpy respectively. Turbulent heat flux vector represents the turbulent convection of fluctuating internal energy or enthalpy by velocity fluctuations. This correlation is modeled as per gradient diffusion hypothesis by considering it proportional to the mean temperature gradient. The proportionality constant is written in terms of eddy viscosity μ_t and turbulent Prandtl number Pr_t [3].

Morkovin's hypothesis applicable for compressible boundary layer suggests that the velocity-temperature correlation coefficient $R_{uT} = -1$ which implies a Pr_t value of 1 [4]. RANS models consider a constant value of $Pr_t = 0.89$ for modeling turbulent heat flux in

† Graduate student, Indian Institute of Technology Bombay

‡ Associate Professor, Indian Institute of Technology Bombay

boundary layer flows. It is to be noted that the basis for Morkovin's hypothesis relies on the fact that the total temperature fluctuations are small in the flow field. The upstream turbulent fluctuations interacting with the shock, make it oscillate about a mean position and the total temperature fluctuation across such a shock wave is of significant level [5]. This indicates to a varying Pr_t value across the shock and in the past varying Pr_t RANS models have shown improved heat flux results in shock dominated flows [2].

The objective in this work is to study the generation of the turbulent heat flux correlation as the flow passes through the shock wave. For this study, we consider the canonical form of homogeneous isotropic turbulence interacting with a normal shock. The turbulence is purely vortical with no temperature, pressure or density fluctuations and is carried by a 1-D uniform mean flow. This isolates the effect of turbulence on the shock without getting in additional complexities such as boundary layer gradient, streamline curvature, flow separation etc. Extensive DNS data [6] is also available for this simplified case thus providing significant insight into essential physics of the problem. A theoretical tool called Linear Inviscid Analysis (LIA) is used for studying this problem.

LIA models the upstream turbulence as combination of 2-D planar disturbance waves [7]. Each of these waves is considered to interact independently with the shock, generating disturbances that could be vortical, acoustic and entropic in nature. The wave properties behind the shock are obtained by solving the linear Euler equations in the downstream regime with the linear Rankine-Hugoniot equations applied at the shock boundary. The overall downstream turbulence is a linear superposition of the results obtained for these independent interactions [5].

Using LIA we study the generation of the streamwise turbulent heat flux $\overline{u'T'}$ across a shock. The DNS data is available for cases with upstream flow having different mean Mach number, turbulent Mach number and Reynolds number upstream of the shock. The correlation coefficient R_{uT} obtained downstream of the shock is studied for these cases of varying M_t and Re_λ and compared with LIA. Finally, the effect of an upstream turbulence spectrum on the generation of the post-shock correlation coefficient is also studied.

2. Flow description

A steady, one-dimensional uniform mean flow is considered upstream and downstream of a normal shock. The mean flow upstream of the shock carries a purely vortical turbulence which is homogeneous and isotropic in nature. The shock distorts from its mean position due to the presence of upstream turbulence. The shock in turn amplifies the turbulence as it passes through it.

For the purpose of theoretical analysis, the shock distortion from its mean position is described by a distance $\xi(y, z, t)$ (see figure 1). The temporal derivative of the shock deviation given by ξ_t represents the streamwise velocity of the shock wave. The transverse derivatives ξ_y and ξ_z denote the angular deviation of the shock in $x-y$ and $x-z$ planes, respectively, where x , y and z represent the coordinates in the lab frame of reference. The associated velocities are u , v and w , respectively.

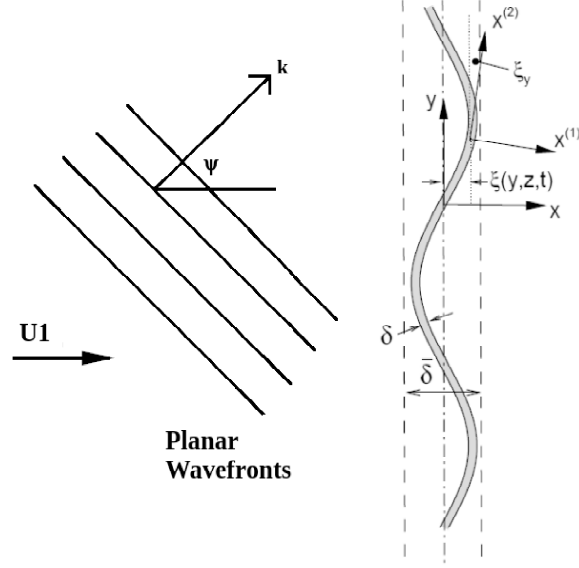


FIGURE 1. Schematic showing a shock wave distorted upon interaction with turbulent fluctuations.

3. Methodology

3.1. LIA formulation

Consider a two-dimensional plane vortical wave of the form given below

$$\frac{u'_1}{U_1} = l A_v e^{ik(mx+ly-U_1mt)} \quad (3.1)$$

$$\frac{v'_1}{U_1} = -m A_v e^{ik(mx+ly-U_1mt)} \quad (3.2)$$

$$p'_1 = T'_1 = \rho'_1 = 0 \quad (3.3)$$

u' and v' representing fluctuations in the streamwise and transverse directions. p' , T' and ρ' represent the fluctuations in pressure, temperature and density, respectively. Also, $m = \cos \psi$ and $l = \sin \psi$ where ψ is the angle between wave number vector and the mean flow direction as shown in figure 1. A_v and k represent the complex amplitude and the wave number of the upstream vorticity wave.

Upon interaction of this single vorticity wave with the shock, three waves are generated. Those are the acoustic, vorticity and entropy waves. The acoustic wave has its contribution to pressure, velocity, temperature and density. The entropy wave has its contribution to temperature and density. The vorticity wave has its contribution only to velocity. Therefore, the waveforms downstream of the shock can be written as

$$\frac{u'_2}{U_1} = F e^{i\bar{k}x} e^{ik(ly-mU_1t)} + G e^{ik(mrx+ly-mU_1t)} \quad (3.4)$$

$$\frac{v_2'}{U_1} = He^{i\tilde{k}x} e^{ik.ly-mU_1t} + Ie^{ik(mrx+ly-mU_1t)} \quad (3.5)$$

$$\frac{T_2'}{\bar{T}_2} = \frac{\gamma-1}{\gamma} Ke^{i\tilde{k}x} e^{ik.ly-mU_1t} + Qe^{ik(mrx+ly-mU_1t)} \quad (3.6)$$

$$\frac{\rho_2'}{\bar{\rho}_2} = \frac{K}{\gamma} e^{i\tilde{k}x} e^{ik.ly-mU_1t} + Qe^{ik(mrx+ly-mU_1t)} \quad (3.7)$$

$$\frac{p_2'}{\bar{p}_2} = Ke^{i\tilde{k}x} e^{ik.ly-mU_1t} \quad (3.8)$$

where F , H and K represent the magnitude of acoustic components related to the streamwise velocity fluctuation, stream-normal velocity fluctuation and pressure fluctuation. G and I represent the contribution from the vorticity wave to the streamwise velocity fluctuation and stream-normal velocity fluctuation. Q represents the contribution of the entropy wave to both temperature and density fluctuation. Also, \tilde{k} represents the wave number of the generated acoustic wave. The streamwise wave number of the downstream vorticity and entropy wave is amplified by a factor r which is the density ratio, $\bar{\rho}_2/\bar{\rho}_1$.

The wave characteristics associated with the shock are given by

$$\frac{\xi_t}{U_1} = Le^{ik.ly-mU_1t} \quad (3.9)$$

$$\xi_y = -\frac{l}{m} Le^{ik.ly-mU_1t} \quad (3.10)$$

where ξ_t and ξ_y represent the shock speed and shock distortion. The boundary condition at the shock is given by the linearised Rankine-Hugoniot(R-H) equations.

$$\frac{u_2' - \xi_t}{U_1} = B_1 \left(\frac{u_1' - \xi_t}{U_1} \right) \quad (3.11)$$

$$\frac{v_2'}{U_1} = \frac{v_1'}{U_1} + E_1 \xi_y \quad (3.12)$$

$$\frac{\rho_2'}{\bar{\rho}_2} = C_1 \left(\frac{u_1' - \xi_t}{U_1} \right) \quad (3.13)$$

$$\frac{p_2'}{\bar{p}_2} = D_1 \left(\frac{u_1' - \xi_t}{U_1} \right) \quad (3.14)$$

B_1 , C_1 , D_1 and E_1 are the functions of the upstream Mach number given by

$$B_1 = \frac{(\gamma-1)M_1^2 - 2}{(\gamma+1)M_1^2}$$

$$C_1 = \frac{4}{(\gamma-1)M_1^2 + 2}$$

$$D_1 = \frac{4\gamma M_1^2}{2\gamma M_1^2 - (\gamma - 1)}$$

$$E_1 = \frac{2(M_1^2 - 1)}{(\gamma + 1)M_1^2}$$

The governing equations downstream of the shock are the linearised Euler equations.

In order to solve for the complex amplitudes, F , H , K , G , I , Q and L , we substitute the downstream waveforms, (3.4 – 3.8) in the linearised R-H and Euler equations to get a set of linear algebraic equations which can be easily solved. The solutions are

$$\tilde{L} = \frac{-m - \beta D_1 l + \frac{mr}{l}[-\alpha D_1 l + B_1 l]}{E_1 \frac{l}{m} - \beta D_1 - \frac{mr}{l}(1 - B_1 + \alpha D_1)} \quad (3.15)$$

$$\tilde{K} = D_1(1 - \tilde{L}) \quad (3.16)$$

$$\tilde{F} = \alpha \tilde{K} \quad (3.17)$$

$$\tilde{H} = \beta \tilde{K} \quad (3.18)$$

$$\tilde{G} = \tilde{L}(1 - B_1 + \alpha D_1) - \alpha D_1 l + B_1 l \quad (3.19)$$

$$\tilde{I} = -\frac{mr}{l} \tilde{G} \quad (3.20)$$

$$\tilde{Q} = -\frac{\tilde{K}}{\gamma} + C_1(l - \tilde{L}) \quad (3.21)$$

The tilde on the complex variables represents normalization by A_v . For example, $\tilde{L} = \frac{L}{A_v}$. α and β are given by

$$\alpha = \frac{a_2^2}{\gamma U_1^2} \frac{\frac{\tilde{k}}{k}}{m - \frac{\tilde{k}}{kr}}$$

$$\beta = \frac{a_2^2}{\gamma U_1^2} \frac{l}{m - \frac{\tilde{k}}{kr}}$$

Thus, for a single vorticity wave upstream of the shock having the wave number k at an angle ψ to the streamwise direction, the downstream properties can be calculated using (3.4)-(3.8) with the aid of solutions (3.15)-(3.21).

Turbulent statistics being an important measure of any turbulent field, can be derived from downstream waveforms. For example, the statistics associated with the streamwise velocity fluctuation downstream of the shock can be calculated as

$$\overline{u_2'^2} = \overline{u_2' u_2'^*} \quad (3.22)$$

where the over-bar implies averaging in the transverse direction and in time. * denotes a complex conjugate. Using (3.4), we get

$$\frac{(\overline{u_2'^2})_{2D}}{U_1^2} = [|\tilde{F}|^2 e^{i(\tilde{k}-\tilde{k}^*)x_+} + |\tilde{G}|^2 + \tilde{F}\tilde{G}^* e^{i(\tilde{k}-kmr)x} + \tilde{F}^*\tilde{G} e^{-i(\tilde{k}^*-kmr)x}] |A_v|^2 \quad (3.23)$$

which is the streamwise component of the turbulent kinetic energy. The subscript '2D' indicates the value for a single wave analysis. The downstream turbulent energy flux $\overline{u_2'T_2'}$ can also be written in a similar way as

$$\left(\overline{u_2'T_2'}\right)_{2D} = 0.5 \left(\overline{u_2'T_2'^*} + \overline{u_2'^*T_2'}\right) \quad (3.24)$$

The values of the above expression can be calculated using (3.4) and (3.6).

The upstream turbulence is modeled as a collection of waves with a 3D energy spectrum tensor

$$E(k) \sim \left(\frac{k}{k_o}\right) e^{-2\left(\frac{k}{k_o}\right)^2} \quad (3.25)$$

where k is the upstream wave number and k_o is the peak wave number. It can be further shown from the analysis that $|A_v|^2$ can be written as

$$|A_v|^2 = \frac{E(k)}{4\pi k^2}$$

For a given upstream spectrum of waves, the total turbulent statistics downstream can be calculated by integrating single wave analysis results over all wave numbers and angles of incidence. Therefore, we obtain

$$\left(\overline{u_2'T_2'}\right)_{3D} = 4\pi \int_{k=0}^{\infty} \int_{\psi=0}^{\frac{\pi}{2}} \left(\overline{u_2'T_2'}\right)_{2D} k^2 \sin \psi \, d\psi \, dk$$

3.2. DNS data

Larsson et al. [6] carried out DNS for the case of purely vortical turbulence interacting with a normal shock. Simulations were performed for 20 cases, each varying in either upstream Mach number, turbulent Mach number or Reynolds number. The upstream Mach number considered ranged from 1.06 to 6. The turbulent Mach numbers for these cases were between 0.15 and 0.38. Further, two cases of upstream Reynolds number based on Taylor-scale, have been considered in this study. These cases highlight the effect of shock strength, upstream turbulent intensity and viscous mechanisms on the shock-turbulence interaction.

Table 1 displays the DNS cases whose data sets have been used for the current study. The number of grid points used for each of the cases are also highlighted. For example, for the case of $M = 1.05$, the grid size is 828×384^2 where the domain consists of 828 points in x-direction and 384 points in y and z directions each. For the case of $Re_\lambda = 75$, a higher number of grid points has been used as the scales of turbulence are smaller and the domain needs to be better resolved. The time dependent solution obtained from the DNS is averaged over a finite time interval to give turbulent statistics for each of these cases. The number of time steps over which the averaging is performed is displayed for the individual cases.

A quantity of interest with respect to DNS data is the dissipation length scale denoted by L_ϵ . The length scale of turbulence at which dissipation of turbulent kinetic energy occurs is given by

M	M_t	Re_λ	Grid size	Time-steps considered for averaging
1.05	0.05	40	828×384^2	128
1.28	0.15	40	1040×384^2	64
1.50	0.15	40	1040×384^2	8
1.87	0.22	40	1257×384^2	8
2.50	0.22	40	1257×384^2	8
3.50	0.16	40	1257×384^2	8
4.70	0.23	40	1257×384^2	8
6.00	0.23	40	1257×384^2	8
1.50	0.14	75	2234×1024^2	48
1.50	0.22	75	2234×1024^2	48
1.50	0.38	75	2366×1024^2	48
3.50	0.15	75	2234×1024^2	48

TABLE 1. List of DNS cases used in the present study.

$$L_\epsilon = (R_{kk}/2)^{3/2}/\epsilon$$

where R_{kk} and ϵ represent twice the turbulent kinetic energy and dissipation rate respectively. This scale is adopted for x-directional normalization while plotting quantities of interest along the domain length x . In the present theoretical study, the peak upstream wavenumber for the incoming turbulence is taken as $k_o = 4$. x can be normalized by dividing with the wavelength of the peak wavenumber ($\lambda_o = 2\pi/k_o$). Also, $k_o \times L_\epsilon$ is a quantity that relies on the shape of the spectrum. For theoretical analysis, a value of $k_o \times L_\epsilon \sim 3 - 4$ can be considered. From this expression also, an equivalent L_ϵ can be obtained to normalize along the x-direction.

4. Results

For a purely vortical upstream turbulence, a finite correlation between velocity and temperature fluctuations is obtained downstream of the shock. The velocity temperature correlation namely R_{uT} is given by

$$R_{uT} = \frac{\overline{u'T'}}{\sqrt{\overline{u'^2}}\sqrt{\overline{T'^2}}}$$

The evolution of R_{uT} as per LIA is shown for two upstream Mach numbers in figure 2. $x = 0$ represents the shock location.

For $M = 1.5$, just downstream of the shock, R_{uT} takes a negative value and rises to have a positive transient peak. Further, in the far-field, a steady positive R_{uT} value is obtained. A similar trend is seen for the $M = 3.5$ case except that the value just downstream of the shock is positive. Acoustic fluctuations are generated behind the shock and they decay with distance from the shock. The transient nature of the R_{uT} variation can be attributed to this phenomenon as velocity and temperature fluctuations both have acoustic components associated with them. For a higher Mach number, a higher value of the far-field correlation coefficient is obtained.

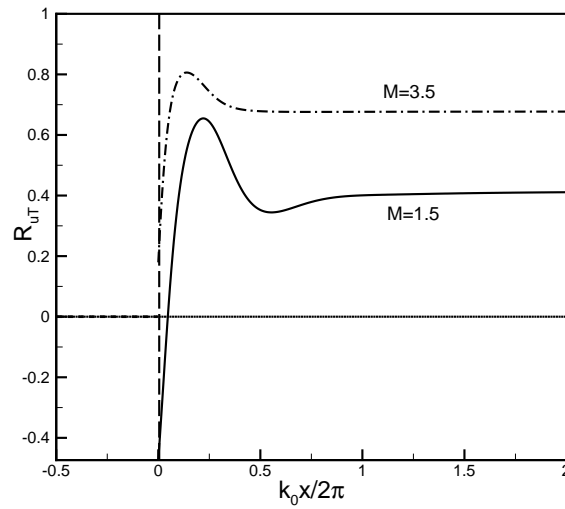


FIGURE 2. Variation of R_{uT} with downstream distance x obtained from LIA.

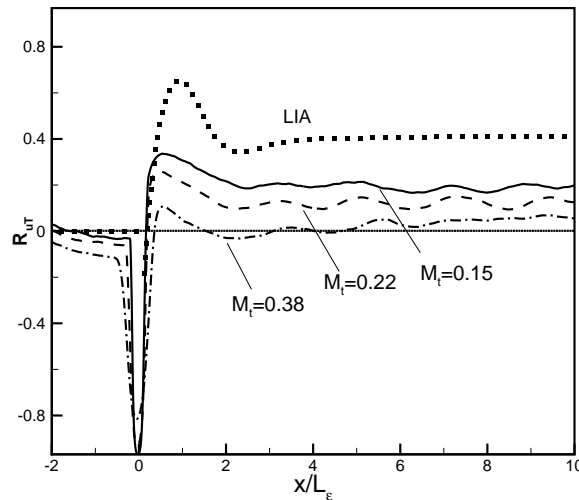


FIGURE 3. Comparison between LIA and DNS for the R_{uT} evolution behind the shock; Upstream Mach number $M = 1.5$.

Figure 3 also shows the generation of R_{uT} in the region downstream of the shock. DNS and LIA results are compared for an upstream Mach number $M = 1.5$. Three different upstream M_t values are taken from the available DNS data sets for comparison. Similar to the linear theory results, DNS also shows a negative near-field R_{uT} just downstream of the shock, followed by a transient peak and a fairly constant far-field value. As the upstream M_t is decreased, the R_{uT} values head closer towards the LIA result. This corroborates with the fact that LIA is applicable for fluctuations of small magnitude as compared to corresponding mean variables.

As per linear theory, $R_{uT} = 0$ in the region upstream of the shock where only vorti-

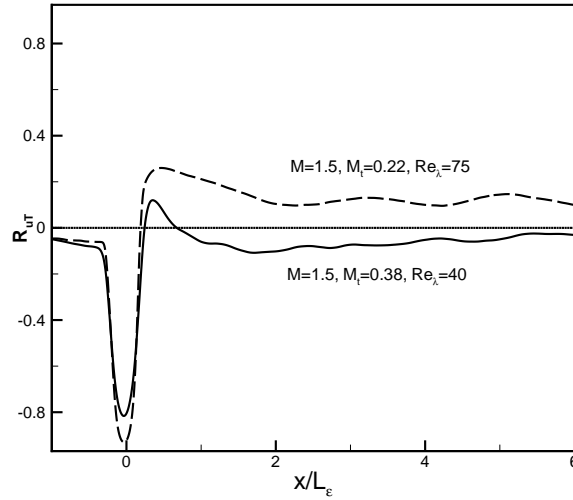


FIGURE 4. Variation of R_{uT} with downstream distance x obtained from DNS showing the difference in far-field R_{uT} evolution for different cases.

cal disturbance is assumed. The upstream flow in the DNS is also meant to have only vortical fluctuations. However, due to acoustics that are unphysical, there also exist temperature fluctuations yielding a finite negative R_{uT} upstream of the shock (see figure 3). This happens especially for higher M_t values and influences the downstream R_{uT} predictions.

Figure 4 shows the variation of R_{uT} along x for Mach number $M = 1.5$ at two different M_t values. As seen, for the case of $M_t = 0.22$, the R_{uT} values beyond the transient peak attain a fairly constant mean value, displaying some oscillations in the downstream region. However, for the case of $M_t = 0.38$, it can be seen that although a sinusoidal pattern is obtained post the transient peak, the trend rises steadily along x . The reason for this steady increase in the oscillation is unknown and needs further probing.

Based on this analysis, a single far-field R_{uT} value cannot be assigned for each case. A mean value can be obtained by averaging all R_{uT} values between $x/L_\epsilon \sim 2$ and the end of the domain. The maximum and minimum R_{uT} values in this span are considered in defining the error bar. Figure 5 shows one such case where maximum, minimum and the average value of R_{uT} have been displayed.

Figure 6 shows the LIA result for near-field and far-field R_{uT} for varying upstream Mach numbers. The near-field R_{uT} for low upstream Mach number takes negative values and asymptotes to a steady positive value for $M \rightarrow \infty$. The far-field R_{uT} also displays a similar trend. It remains negative only for a very small range of upstream Mach numbers close to unity. For higher Mach numbers, the R_{uT} value is close to 0.7. From the figure, the far-field value of R_{uT} is higher than the near-field value for all upstream Mach numbers. This increase along x -direction in the post-shock region can be attributed to the decay of acoustic fluctuations generated behind the shock.

Figure 7 shows the variation of the far-field R_{uT} with the upstream Mach number. DNS and LIA results are compared and the effect of the upstream Reynolds number on R_{uT} is shown. R_{uT} as predicted by DNS also shows negative values for very low upstream Mach numbers and reaches as steady positive value for higher Mach numbers. The DNS

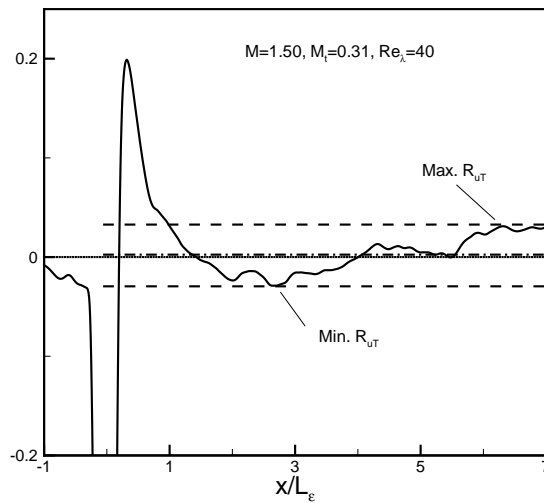


FIGURE 5. Variation of R_{uT} with downstream distance x obtained from DNS for a single case showing the maximum, minimum and average R_{uT} .

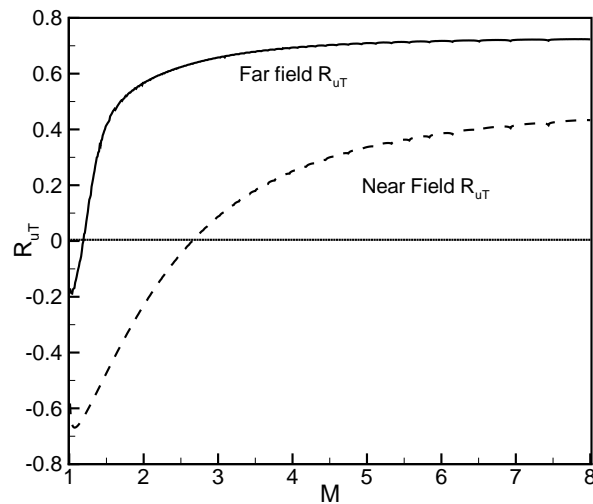


FIGURE 6. Variation of R_{uT} with upstream Mach number M for near-field and far-field obtained from LIA.

study considers two upstream Reynolds numbers based on Taylor micro-scale, namely $Re_\lambda = 40$ and $Re_\lambda = 75$. For the same upstream Mach number, R_{uT} corresponding to $Re_\lambda = 75$ yields a higher positive value as compared to $Re_\lambda = 40$. LIA gives a much higher value of R_{uT} as compared to DNS. It is to be noted that LIA is based on inviscid theory and formulations are for the limiting case of $Re \rightarrow \infty$ ignoring the effect of viscosity.

The form of the energy spectrum in the LIA formulation representing the upstream isotropic turbulence is seen in (3.25). The spectrum however is appropriate for low

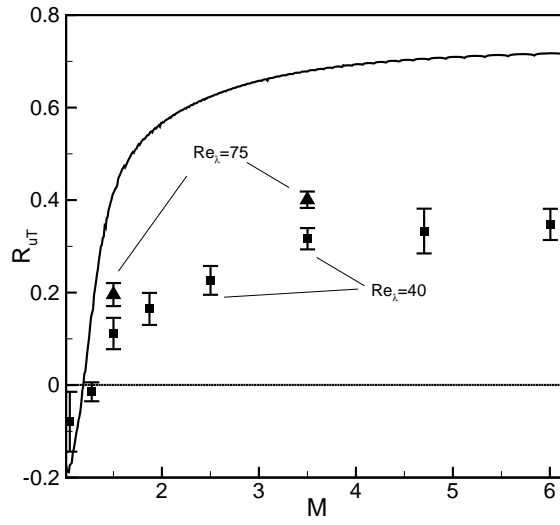


FIGURE 7. Comparison between LIA and DNS results for far-field R_{uT} for varying upstream Mach number M .

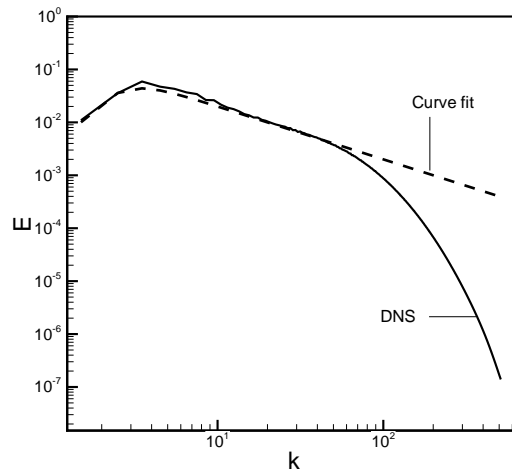


FIGURE 8. Energy spectrum obtained from DNS for the case of $Re_{\lambda} = 75$ and its curve-fit.

Reynolds numbers. In the recent DNS simulations, the energy spectrum obtained for the case of $Re_{\lambda} = 75$ is shown in figure 8.

The curve-fit for this spectrum has the form

$$E(k) \sim \frac{k^4}{(k^4 + 35)^{1.25}}$$

Figure 9 shows the variation of R_{uT} along the x direction for a single upstream Mach number of $M = 1.5$.

Both spectra are implemented in the theory and their effect on the R_{uT} generation down-

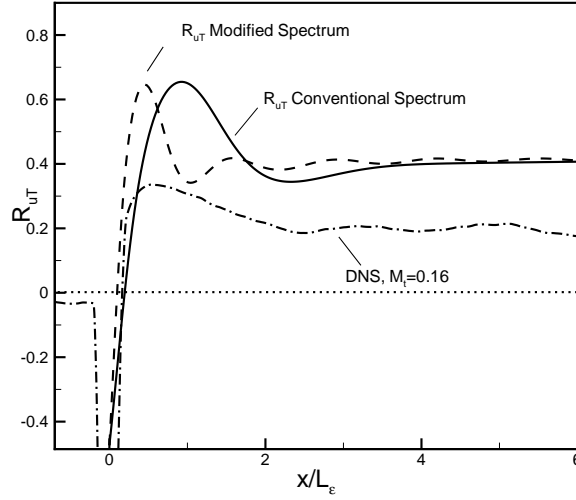


FIGURE 9. Figure shows the effect of upstream spectrum on variation of R_{uT} along x direction. The upstream Mach number is $M = 1.5$.

stream of the shock is shown. Also shown is the R_{uT} variation as per DNS for a case of low upstream M_t value. The modified spectrum reveals an early decay of acoustic fluctuations as compared to the conventional spectrum result and the DNS case. However, the transient peak and the far-field R_{uT} for both the cases of LIA have similar values. This shows that for theoretical analysis, the spectrum shape has no effect on the far-field R_{uT} value, but only on the nature of the acoustics generated behind the shock.

5. Conclusions

The generation of the turbulent heat flux across a normal shock was studied. The turbulence upstream of the shock was considered to be purely vortical. For low upstream Mach numbers, LIA predicted negative R_{uT} just behind the shock. However, the value of R_{uT} reaches a steady positive value after passing through a transient peak value. For high Mach numbers, the LIA predicts a similar trend, except that the post-shock value of R_{uT} was positive.

A fairly good qualitative match was obtained in the comparison with DNS data. However, LIA over-predicted the R_{uT} value for the entire downstream region. An analysis of appropriate cases of DNS showed that R_{uT} values were sensitive to the upstream turbulent Mach number M_t and Taylor-scale Reynolds number Re_λ . For low M_t values and higher Re_λ values, the DNS values approached towards theoretical predictions.

Turbulent heat flux vector modeling in the RANS framework is based on the assumption that $R_{uT} \sim -1$. A positive value of R_{uT} in the far-field indicated towards exploring alternate RANS modeling strategies for similar flows. It was also seen from the theory that a change in the upstream energy spectrum shape, only altered the acoustic generation downstream of the shock and had no effect on far-field R_{uT} values.

Acknowledgments

Financial support has been provided by the German Research Foundation (Deutsche Forschungsgemeinschaft – DFG) in the framework of the Sonderforschungsbereich Transregio 40. The authors wish to thank Professor Johan Larsson of the University of Maryland for useful discussions and DNS data.

References

- [1] ROY, C. J. AND BLOTTNER, F. G. (2001). Review and assessment of turbulence models for hypersonic flows. *Progress in Aerospace Sciences*, **42**, 469–530.
- [2] XIAO, X. AND HASSAN, H. A. (2007). Modeling scramjet flows with variable turbulent Prandtl and Schmidt numbers. *AIAA Journal*, **45**, 1415–1423.
- [3] WILCOX, D. C. (Ed.) (2000) *Turbulence Modeling for CFD*. DCW Industries
- [4] MORKOVIN, M. V. (1962). Effects of compressibility on turbulent flows. *Mecanique de la Turbulence*, 367–380.
- [5] MAHESH, K., LELE, S. K. AND MOIN, P. (1996). *The interaction of a shock wave with a turbulent shear flow*. Thermosciences division, Department of Mechanical Engineering, Stanford University, Report No. TF-69, Stanford, CA.
- [6] LARSSON, J., BERMEJO-MORENO, I. AND LELE, S. K. (2013). Reynolds-and Mach number effects in canonical shock-turbulence interaction. *Journal of Fluid Mechanics*, **717**, 293–321.
- [7] KOVASZNAVY, L. S. G. (1953). Turbulence in supersonic flow. *J. Aeronaut. Sci.*, **20**, 657–682.
- [8] SINHA, K. (2012). Evolution of enstrophy in shock/homogeneous turbulence interaction. *Journal of Fluid Mechanics*, **707**, 74–110.
- [9] MAHESH, K., LELE, S. K. AND MOIN, P. (1997). The influence of entropy fluctuations on the interaction of turbulence with a shock wave. *Journal of Fluid Mechanics*, **334**, 353–379.

